

the present results are in good agreement with those reported by Ramanathan and Kumar. However, a significant deviation can be found for the case of  $A = 1$ . The main reason is due to the influence of heat transfer between the fluid inside the solid enclosure and the enclosure wall, resulting in a lower maximum dimensionless temperature on the channel surface in their results.

### Induced Reynolds Number

A generalized derivation of the induced mass flow rate for the fully developed limit of natural convection in a vertical long channel with asymmetric isoflux heating was presented by Hung et al.<sup>3</sup> Accordingly, the fully developed limit of modified induced Reynolds number in a vertical channel with symmetrical isoflux heating can be expressed as

$$Re^* = \sqrt{\frac{T}{12}} Ra^{-0.5} \quad (11)$$

where  $Re^*$  is defined as  $Re^* = Q/Gr$ , with  $Q$  denoting the dimensionless induced flow rate in the channel, i.e.

$$Q = \int_0^1 U dY$$

and  $Gr$  as defined in Eq. (1).

From the scale analysis, the modified induced Reynolds number of a vertical long plate was found to be inversely proportional to the 0.6 power of Rayleigh number.<sup>6</sup> By checking with the present results, the single plate limit of the modified induced Reynolds number can be quantitatively expressed as

$$Re^* = 0.5 Ra^{-0.6} \quad (12)$$

Similar to the method suggested by Churchill and Usagi<sup>7</sup> for correlating a composite Nusselt number, a new composite  $Re^*$  correlation for a vertical channel having arbitrary channel spacing is proposed as

$$Re^* = [(\sqrt{\frac{T}{12}} Ra^{-0.5})^{-6} + (0.5 Ra^{-0.6})^{-6}]^{-1/6} \quad (13)$$

As indicated in Fig. 3, the data from the present study are very consistent with the results of the boundary-layer analysis presented by Miyatake and Fujii,<sup>8</sup> except for  $A = 1$ . This shows that the vertical heat conduction in the channel and free space stratification near the channel have a significant effect on the induced Reynolds number when the channel aspect ratios are small.

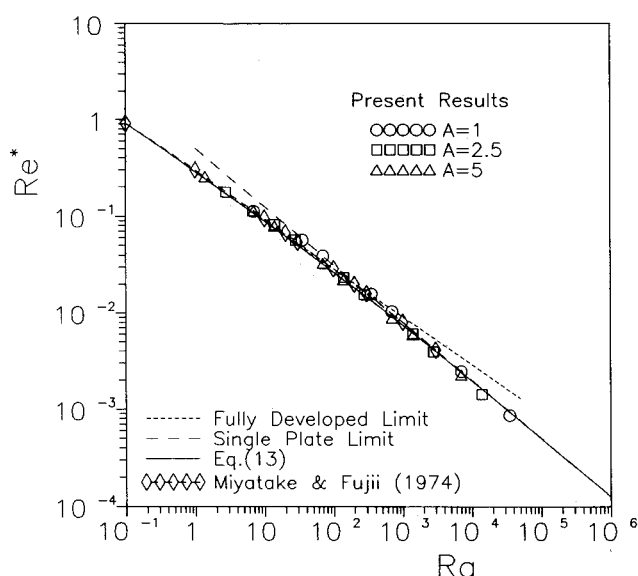


Fig. 3 Relationship between induced Reynolds number and Rayleigh number.

### Conclusions

The main conclusions from the present results can be summarized as follows:

1) For small channel aspect ratios and low Rayleigh numbers, significant deviations of the Nusselt number and maximum temperature distributions exist between the present results and the predications from the existing long-channel correlations. This discrepancy is due to the fact that the effects of vertical thermal diffusion in the channel and free space stratification near the channel are significant.

2) A new correlation of the induced Reynolds number for a vertical finite-length isoflux channel is proposed.

### References

- Ramanathan, S., and Kumar, R., "Correlations for Natural Convection Between Heated Vertical Plates," *Journal of Heat Transfer*, Vol. 113, Feb. 1991, pp. 97–107.
- Van Doormaal, J. P., and Raithby, G. D., "Enhancement of the SIMPLE Method for Predicting Incompressible Fluid Flow," *Numerical Heat Transfer*, Vol. 7, No. 2, 1984, pp. 147–163.
- Hung, Y. H., Lu, C. T., and Perng, S. W., "A Composite Nu Correlation for Natural Convection in Vertical Finite-Length Channels with Asymmetric Isoflux Heating," *Proceedings of the 3rd ASME-JSME Thermal Engineering Joint Conference*, Vol. 1, March 1991, pp. 151–161.
- Bar-Cohen, A., and Rohsenow, W. M., "Thermally Optimum Spacing of Vertical, Natural Convection Cooled, Parallel Plates," *Journal of Heat Transfer*, Vol. 106, Feb. 1984, pp. 116–123.
- Wirtz, R. A., and Stutzman, R. J., "Experiments on Free Convection Between Vertical Plates with Symmetric Heating," *Journal of Heat Transfer*, Vol. 104, Aug. 1982, pp. 501–507.
- Bejan, A., *Convection Heat Transfer*, Wiley-Interscience Publication, New York, 1984, pp. 114–133.
- Churchill, S. W., and Usagi, R., "A General Expression for the Correlation of Rates of Transfer and Other Phenomena," *AIChE Journal*, Vol. 18, No. 6, 1972, pp. 1121–1138.
- Miyatake, O., and Fujii, T., "Natural Convective Heat Transfer Between Vertical Parallel Plates with Unequal Heat Fluxes," *Heat Transfer-Japanese Research*, Vol. 3, No. 3, 1974, pp. 29–33.

## Prediction of Radiative Transfer from Potential Core of a Hot Jet

Srinath S. Heragu\* and K. V. L. Rao†

Aeronautical Development Agency, Vibhuthipura,  
Bangalore 560 037, India

and

B. N. Raghunandan‡

Indian Institute of Science, Bangalore 560 012, India

### Nomenclature

- $a_\lambda$  = absorption coefficient of species as a function of wavelength  
 $i'_\lambda, i'_{\lambda b}$  = intensity and blackbody intensity at a point in medium as a function of direction and wavelength  
 $R$  = radius of nozzle face

Received Feb. 24, 1993; revision received Aug. 27, 1993; accepted for publication Aug. 31, 1993. Copyright © 1993 by the authors. Published by the American Institute of Aeronautics and Astronautics, Inc., with permission.

\*Scientist, Signature Analysis Group.

†Group Director, Signature Analysis Group.

‡Associate Professor, Department of Aerospace Engineering.

- $r$  = distance from the sensor to the far end of a column  
 $s$  = length of an elemental gas column  
 $\alpha, \beta$  = angles between sensor perpendicular and panel perpendicular (towards nozzle axis) with the line joining panel centroid to sensor center

### Introduction

ONE of the important industrial applications of infrared radiation from gases is related to the jet from rocket and aircraft engines as it dictates the vehicle detectability. This has generated a lot of activity in simulation and analysis of infrared (IR) signatures of aircraft. Decher<sup>1</sup> analyzed IR signatures of a two-dimensional jet, assuming a simple absorption coefficient model for gas radiation. Gauffre<sup>2</sup> presented details of aircraft IR modeling, which also included the IR intensity from plumes. The physical limitations typical of solutions in radiative transfer studies were largely removed by Ludwig et al.,<sup>3</sup> and later extended by others,<sup>4,5</sup> who presented theoretical models for spectral radiance calculation for nonhomogeneous absorbing, emitting, and scattering media. Thynell<sup>6</sup> considered the scattering effect on spectral radiance and heat flux calculations from homogeneous cylindrical plumes, while Chui et al.<sup>7</sup> have presented a finite volume method compatible with fluid flow solvers.

Radiation from hot jets and plumes differs from the above in terms of a noncylindrical gas core, unconfined nature and the consequent mixing processes, and in the sensor location and orientation. The present work, which presents an ab initio modeling of plume radiation, goes a little further in the estimation of heat flux and intensity from a noncylindrical volume of potential core on a sensor located and oriented arbitrarily in space, as shown in Fig. 1a.

### Geometric Modeling

The potential core is a homogeneous and isothermal medium of uniform properties with a reducing cross section along its axis. The task of geometric modeling is involved, as the sensor perceives widely different parts, shapes, and regions of the potential core with respect to its location and orientation. Hence, detailed and exhaustive geometric modeling has been developed to isolate the part of the potential core responsible for heat signals perceived by the sensor. It involves the generation of planar grids on the nozzle face and the outer surface of the potential core. A typical grid pattern on the nozzle face is shown in the inset of Fig. 1a. The lines of sight of the centroids of some of these grid panels, from the sensor center, will form the axes of elemental gas columns which contribute to the radiation. A typical elemental gas column bounded by the far end panel and near end panel is shown in Fig. 1b. The radiation through each of the contributory elemental gas columns results in the heat flux of radiation, while that gas column, containing the perpendicular to the sensor (on its active face), accounts for the intensity of radiation. The isolation of these gas columns requires the isolation of far end panels like AA and CC shown in Fig. 1a, for which  $\alpha$  and  $\beta$  are less than 90 deg, and the isolation of near end panels like DD, for which only  $\alpha$  is less than 90 deg. Panels like BB (also shown in Fig. 1a), for which both or only  $\alpha$  are greater than or equal to 90 deg, are disregarded, as they do not contribute to the perceived radiation.

### Radiation Modeling

The gas mixture is assumed to be a shock-free, absorbing, emitting, and nonscattering medium containing a maximum of three species, like CO<sub>2</sub>, CO, and H<sub>2</sub>O. A simple band radiation model has been applied for band radiation which occurs, because temperatures are not high. The intensity change in a nonscattering medium given as<sup>8</sup>

$$\frac{di'_\lambda}{ds} = a_\lambda(i'_{\lambda b} - i'_\lambda) \quad (1)$$

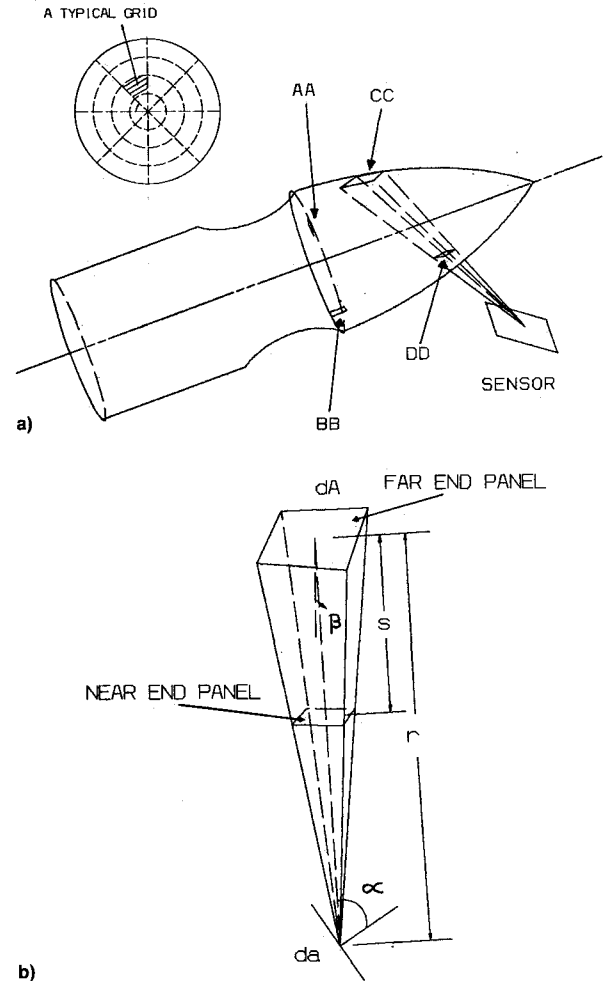


Fig. 1 Typical configuration: a) sensor location and grids on nozzle face and potential core and b) gas column radiating onto sensor.

is integrated (as  $a_\lambda$  is constant in the potential core) to obtain the intensity attenuation through it, as

$$i'_\lambda = i'_{\lambda 0} \exp[-a_\lambda s] + i'_{\lambda b}(1 - \exp[-a_\lambda s]) \quad (2)$$

where  $i'_{\lambda 0}$ , the directional spectral intensity at the beginning of any gas column, is assumed as nil. For a multicomponent mixture,  $a_\lambda$  is replaced by the sum of the absorption coefficients of each species in the mixture. The absorption coefficient  $a_\lambda$  is species dependent and spectral resolution of the data. It is calculated using the exponential band model given by Sparrow and Cess,<sup>9</sup> as

$$a_\lambda = \rho \left( \frac{c_1}{c_2} \right) \left( \frac{100}{T} \right)^n \exp - \left[ \frac{|\nu_0 - \nu|}{c_2} \left( \frac{100}{T} \right)^n \right] \quad (3)$$

where  $\rho$  is the density and  $T$  the temperature of the radiating species,  $c_1$  and  $n$  are constants for a particular species,  $c_2$  is a temperature-based constant for a particular species,  $\nu$  is the wave number, and  $\nu_0$  is the wave number corresponding to the band center. The constants required for this representation have been given in Refs. 8, 10, and 11.

Therefore, the radiation through a typical elemental gas column incident at the sensor location (as shown in Fig. 1b), given by

$$d^3Q = i'_\lambda d\lambda \left[ \frac{(dA) \cos \beta}{r^2} \right] [da \cos(\alpha)] \quad (4)$$

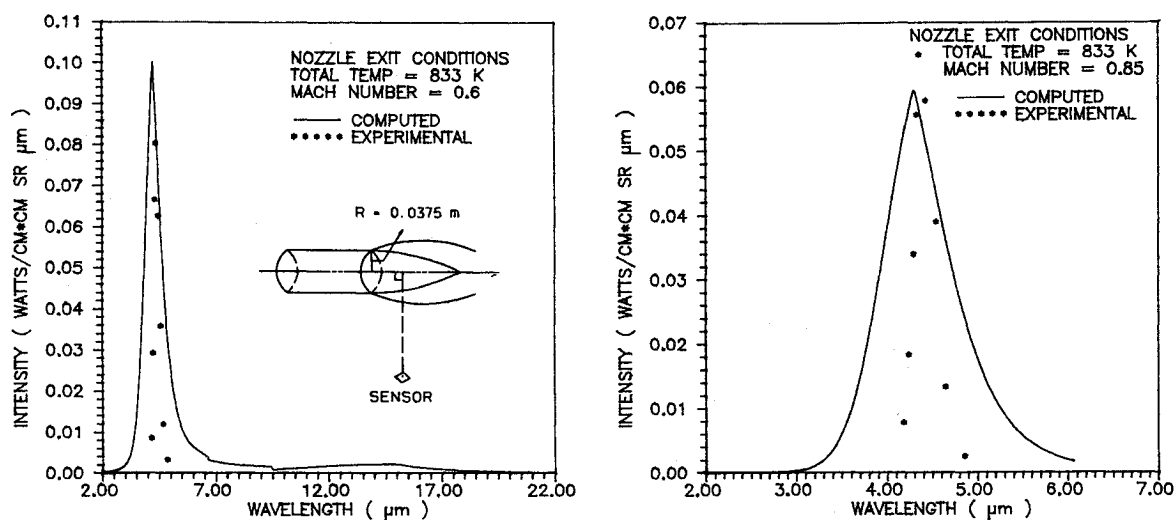


Fig. 2 Spectral intensity variations.

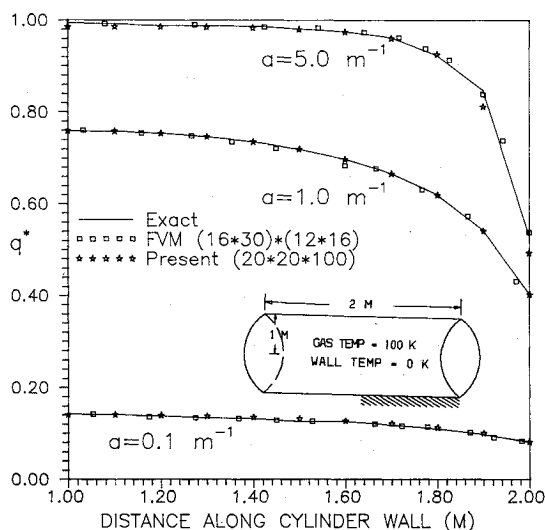


Fig. 3 Radiant heat transfer on the side wall of a cylindrical enclosure containing an absorbing, emitting, and nonscattering gas.

can be numerically integrated over all bands and appropriate solid angle to give the total heat flux  $q$  (radiation per unit area) as

$$q = \frac{dQ}{da} = \sum \left\{ \sum (i'_\lambda d\lambda) \left[ \frac{dA \cos(\beta)}{r^2} \right] \cos(\alpha) \right\} \quad (5)$$

where  $d^3Q$  is the heat transfer rate,  $d\lambda$  is the elemental wavelength interval, and  $dA$  and  $da$  are the elemental areas of the far end panel and sensor, respectively.

### Results and Discussion

Experimental results given by Krishnamoorthy et al.<sup>12</sup> have been used for validation of intensity predictions, which have been made assuming a species concentration (actually mass fraction) of 0.0005, 0.185, and 0.088 for the CO, CO<sub>2</sub>, and H<sub>2</sub>O species, respectively. Figure 2 shows highly favorable agreement with measurements made 1 diameter downstream of the nozzle exit. The signal is higher for the plume with lower Mach number, but higher static temperature. The intensity prediction occurs over a wider band width than it actually is, because of exponential band model. Benchmark-type test cases provided by Chui et al.<sup>7</sup> have been used for validation of heat flux predictions. The present predictions of  $q^*$  (defined as the ratio of actual radiative heat flux from the gray gas column incident on the side wall to that from a blackbody at the same temperature), have been compared

with exact results and predictions of the finite volume method (FVM) of Chui et al. in Fig. 3. The present predictions and the FVM results compare well with the exact results, but the present predictions have been generated with a significantly lesser number of grids ( $20 \times 20 \times 100$ ) than the FVM ( $16 \times 30 \times (12 \times 16)$ ).

### Conclusions

The present work provides a capability to simulate and analyze the IR signature of the potential core of an engine exhaust jet in terms of the intensity and heat flux signals. The good comparison of the predicted results with the experimental ones, and the flexibility allowed by the formulation for any arbitrary jet location and sensor orientation and location, confirms and enhances its utility.

### References

- Decher, R., "Infrared Emissions from Turbofans with High Aspect Ratio Nozzles," *Journal of Aircraft*, Vol. 18, No. 12, 1981, pp. 1025-1031.
- Gauffre, G., "Aircraft Infra-Red Radiation Modeling," *La Recherche Aerospaciale*, No. 4, 1981, pp. 21-41.
- Ludwig, C. B., Malkmus, W., Freeman, G. N., Slack, M., and Reed, R., "A Theoretical Model for Absorbing, Emitting and Scattering Plume Radiation," *Spacecraft Radiative Transfer and Temperature Control*, edited by T. E. Horton, Vol. 83, Progress in Astronautics and Aeronautics, AIAA, New York, 1982, pp. 111-127.
- Nelson, H. F., "Influence of Particulates on Infrared Emission from Tactical Rocket Exhausts," *Journal of Spacecraft and Rockets*, Vol. 21, No. 5, 1984, pp. 425-432.
- Lyons, R. B., Wormhoudt, J., and Gruninger, J., "Scattering of Radiation by Particles in Low-Altitude Plumes," *Journal of Spacecraft and Rockets*, Vol. 20, No. 2, 1983, pp. 189-192.
- Thynell, S. T., "Effect of Linear-Anisotropic Scattering on Spectral Emission from Cylindrical Plumes," *Journal of Thermophysics and Heat Transfer*, Vol. 6, No. 2, 1992, pp. 224-231.
- Chui, E. H., Raithby, G. D., and Hughes, P. M. J., "Prediction of Radiative Transfer in Cylindrical Enclosures with the Finite Volume Method," *Journal of Thermophysics and Heat Transfer*, Vol. 6, No. 4, 1992, pp. 605-611.
- Siegel, R., and Howell, J. R., *Thermal Radiation Heat Transfer*, McGraw-Hill, New York, 1981.
- Sparrow, E. M., and Cess, R. D., *Radiation Heat Transfer*, Brooks/Cole Publishing, Belmont, CA, 1966.
- Edwards, D. K., and Menard, W. A., "Correlations for Absorption by Methane and Carbon Dioxide Gases," *Applied Optics*, Vol. 3, No. 7, 1964, pp. 847-852.
- Edwards, D. K., Flornes, B. J., Glassen, L. K., and Sun, W., "Correlations of Absorption by Water Vapor at Temperatures from 300° to 1100 K," *Applied Optics*, Vol. 4, No. 6, 1965, pp. 715-721.
- Krishnamoorthy, V., and Pai, B. R., "Aerothermodynamics and Infrared Emission Characteristics of Simulated Aeroengine Jet Plumes," Propulsion Div., National Aeronautical Lab., Project Document PR 9113, Bangalore, India, July 1991.